

## Monitoring of phosphatase and kinase activity using $^{31}\text{P}$ NMR

Xiaofan Guo<sup>a</sup>, Bowen Han<sup>a</sup>, Wenhan Qiu<sup>b</sup>, Peiran Deng<sup>c</sup>, Songsen Fu,<sup>\*a</sup> Jianxi Ying,<sup>\*a</sup> Yufen Zhao<sup>a,d</sup>

<sup>a</sup> Institute of Drug Discovery Technology, Ningbo University, Ningbo 315211, Zhejiang, China.

<sup>b</sup> Zhejiang Provincial Key Laboratory of Robotics and Intelligent Manufacturing Equipment Technology, Ningbo Institute of Materials Technology and Engineering, Chinese Academy of Sciences, Ningbo 315201, China.

<sup>c</sup> School of Materials Science and Engineering, Hunan Institute of Technology, Hengyang 421002, China.

<sup>d</sup> Department of Chemical Biology, College of Chemistry and Chemical Engineering, Xiamen University, Xiamen 361005, Fujian, China.

## Supporting Information

### Contents

1. Measurement deviation .....	2
2. $^{31}\text{P}$ NMR spectra of cAMP .....	3
3. $^{31}\text{P}$ NMR spectra of AMP .....	5
4. Thermal stability of cAMP and AMP .....	7
5. PDE II enzyme activity time gradient assay .....	8
6. Time gradient measurement of HK enzyme activity .....	9
7. $^{31}\text{P}$ NMR screening of inhibitors .....	10

## 1 Measurement deviation

**Table S1.** Differentiations between theoretical and experimental concentrations of phosphorus-containing substances. Experimental concentrations were calculated with  $^{31}\text{P}$  NMR calibration curves.

	cAMP		AMP		glucose-6-phosphate	
Theo. (mM)	2	5	2	5	2	5
Exp. (mM)	1.96	4.73	1.91	4.89	1.92	5.46
$\Delta$ diff.	2.0%	5.4%	4.5%	2.2%	4.0%	9.2%

$\Delta$  diff. =  $|\text{Theo.} - \text{Exp.}| \text{ Theo.}^{-1} \cdot *100\%$ . All of the differences are less than 10%.

## 2 <sup>31</sup>P NMR spectra of cAMP

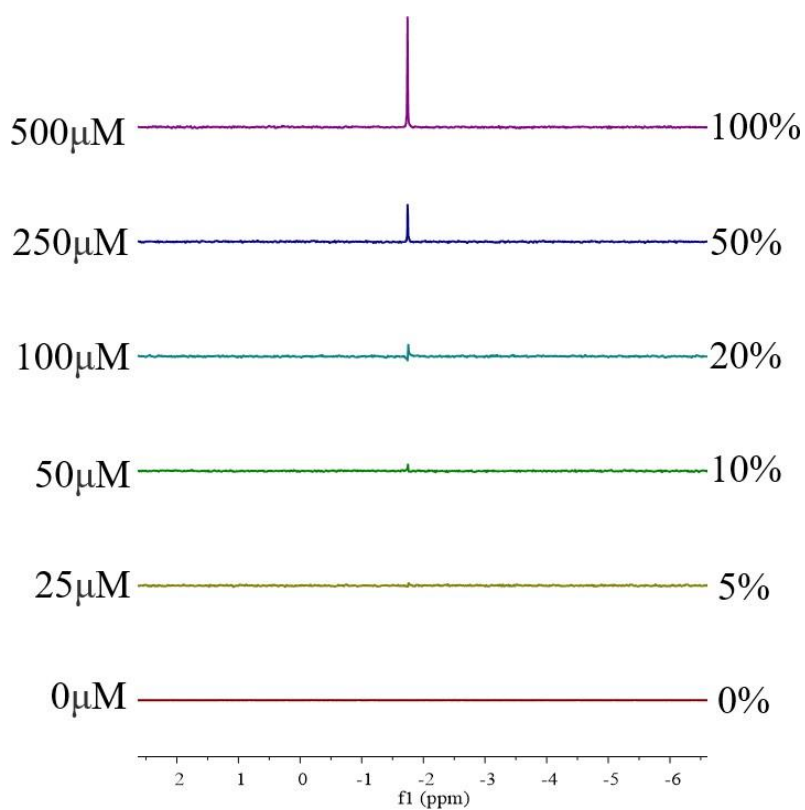


Fig. S1. <sup>31</sup>P NMR spectra of different concentrations of cAMP to quantify the accuracy of cAMP/AMP concentration measurements. 25 μM, 50 μM, 60 μM, 100 μM, 125 μM, 250 μM, and 500 μM cAMP were dissolved in 10% D<sub>2</sub>O, and 500 μM cAMP was converted into 100%, it can be seen from the figure that the peak intensity of cAMP changes with the concentration of cAMP. There is a positive correlation, the higher the concentration of cAMP, the higher the peak, and vice versa.

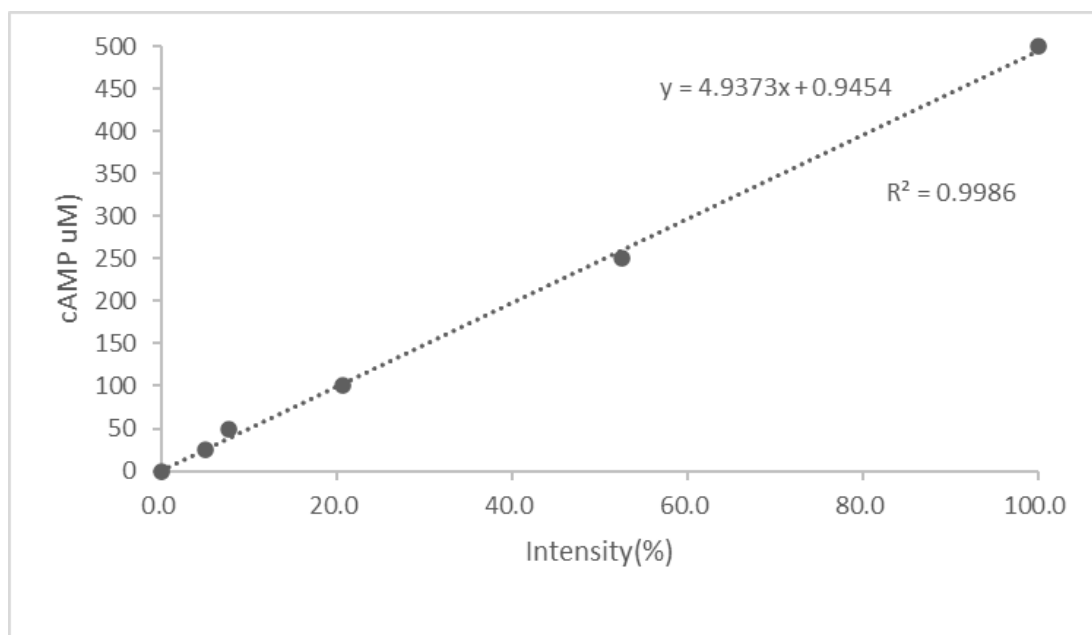


Fig. S2. Calibration curves for different concentrations of cAMP. The peak area of the  $^{31}\text{P}$  NMR spectrum of cAMP with different concentrations in the above figure is the original data, and the cAMP peak area of 500  $\mu\text{M}$  is converted into 100% to obtain the linear relationship between the cAMP concentration and the peak area,  $R^2=0.9986$  indicates the peak area and the concentration. Linear correlation is good. And another two concentrations were used to verify the standard curve, and the error between the experimental value and the real value was within 10%. From the above experimental results, it can be known that the concentration of cAMP can be quickly and accurately obtained by  $^{31}\text{P}$  NMR technology.

### 3 <sup>31</sup>P NMR spectra of AMP

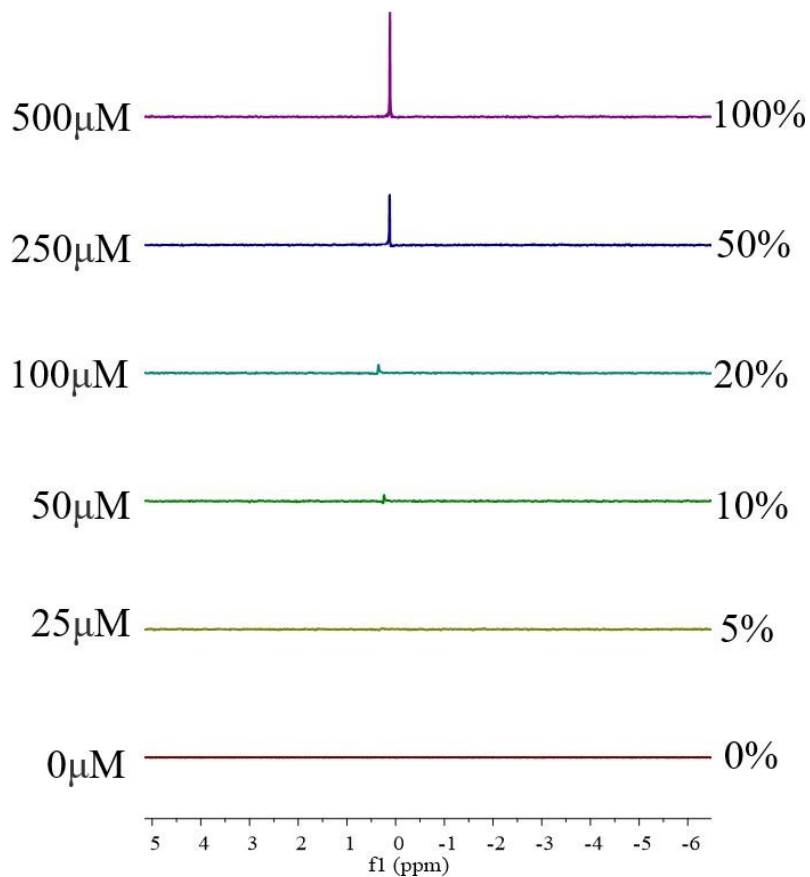


Fig. S3. <sup>31</sup>P NMR spectra of different concentrations of AMP to quantify the accuracy of cAMP/AMP concentration measurements. 25 μM, 50 μM, 60 μM, 100 μM, 125 μM, 250 μM, and 500 μM cAMP were dissolved in 10% D<sub>2</sub>O, and 500 μM AMP was converted into 100%, it can be seen from the figure that the peak intensity of AMP changes with the concentration of AMP. There is a positive correlation, the higher the concentration of AMP, the higher the peak, and vice versa.

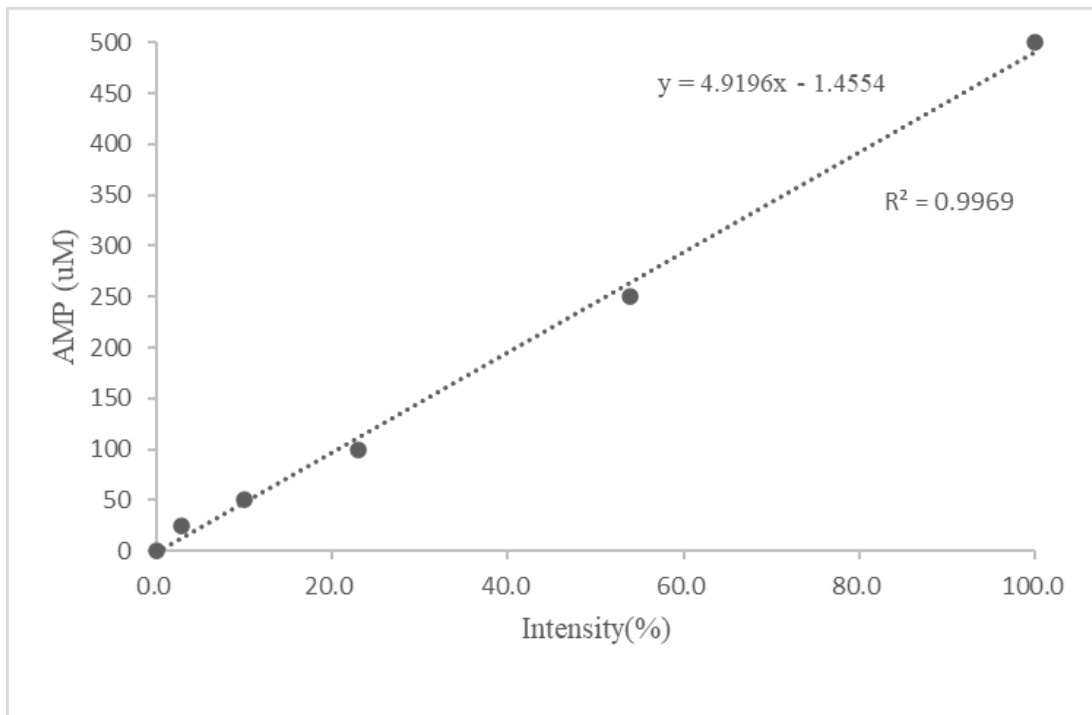


Fig. S4. Calibration curves for different concentrations of AMP. The peak area of the  $^{31}\text{P}$  NMR spectrum of AMP with different concentrations in the above figure is the original data, and the AMP peak area of 500  $\mu\text{M}$  is converted into 100% to obtain a linear relationship between cAMP concentration and peak area.  $R^2=0.9969$  indicates that the peak area and concentration Linear correlation is good. And another two concentrations were used to verify the standard curve, and the error between the experimental value and the real value was within 10%. From the above experimental results, it can be known that the concentration of AMP can be quickly and accurately obtained by  $^{31}\text{P}$  NMR technology.

#### 4 Thermal stability of cAMP and AMP

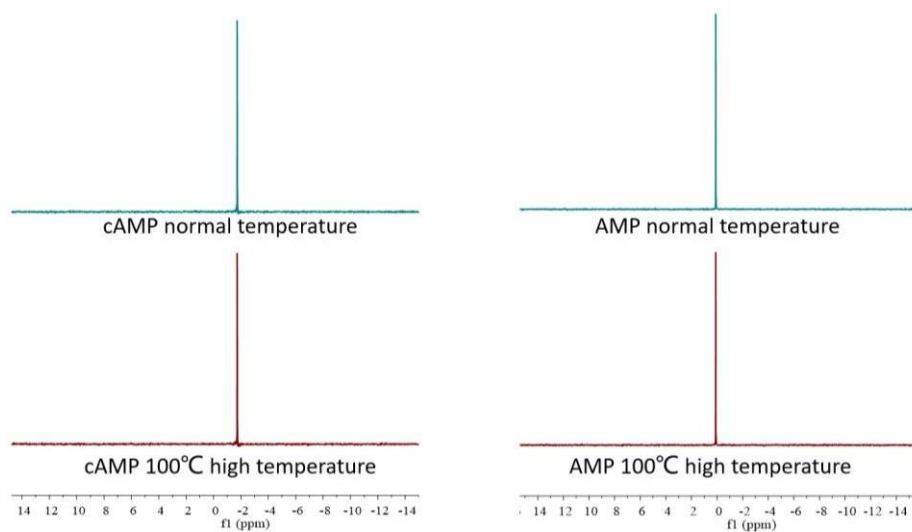


Fig. S5. Thermostability experiments of cAMP and AMP. Since the enzyme needs to be inactivated in this experiment, and high temperature inactivation is used, the thermal stability of the reactants needs to be tested. The cAMP/AMP samples of equal concentration are divided into two parts, and one part is subjected to 5min 100°C inactivation. High temperature treatment, no treatment at room temperature, and  $^{31}\text{P}$  NMR detection found that the peak areas of the samples treated at room temperature and high temperature were unchanged, so short-term high temperature treatment did not affect cAMP/AMP.

## 5 PDE II enzyme activity time gradient assay

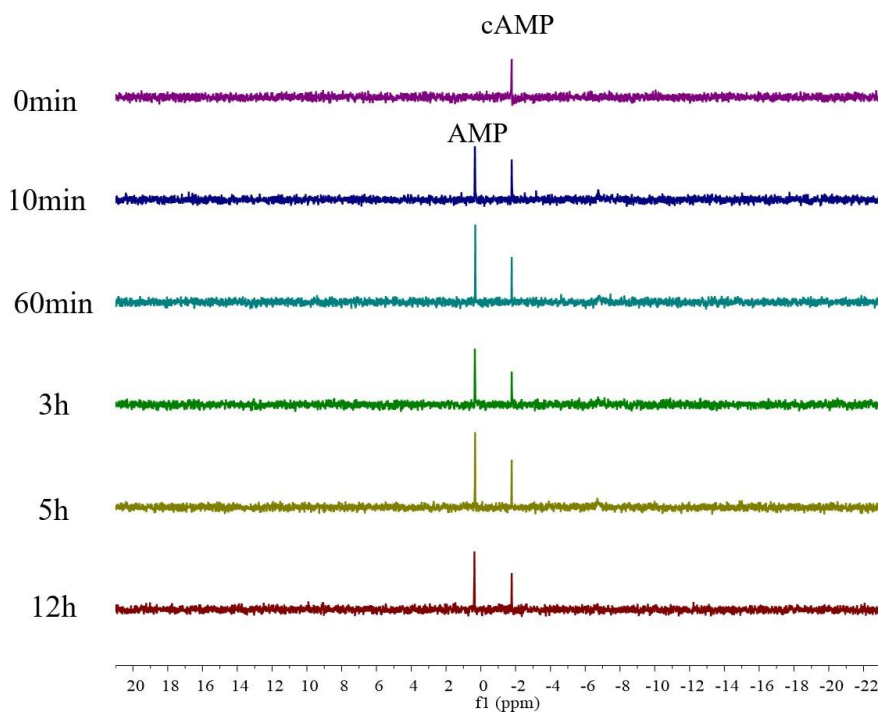


Fig. S6. Enzymatic activity time gradient assay for PDE II. We have analyzed the enzymatic activity of PDE II in real-time by hydrolysis of cAMP or AMP production. Under our experimental conditions, a reaction time of 10 minutes was sufficient to produce detectable amounts of AMP and the amount of substrate or product remained essentially unchanged after 10 minutes.



## 6 Time gradient measurement of HK enzyme activity

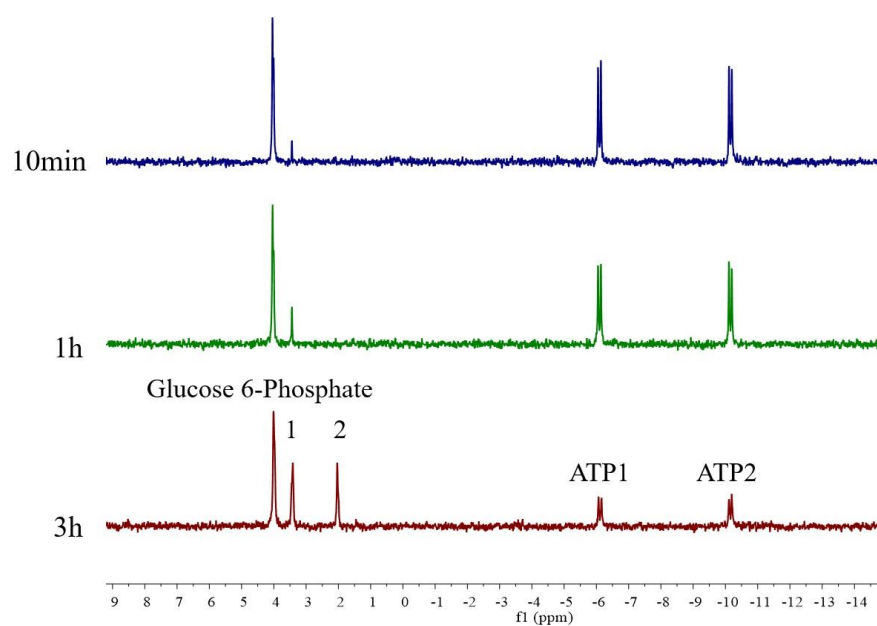


Fig. S7. Enzymatic activity time gradient assay for HK. We analyzed the enzymatic activity of HK in real-time by the production of glucose-6-phosphate. Under our experimental conditions, a reaction time of 3 hours was sufficient to produce detectable amounts of glucose-6-phosphate. Moreover, the enzymatic reaction produces many by-products, but the chemical shifts are all different from glucose-6-phosphate and can be well distinguished.

## $^{31}\text{P}$ NMR screening of inhibitors

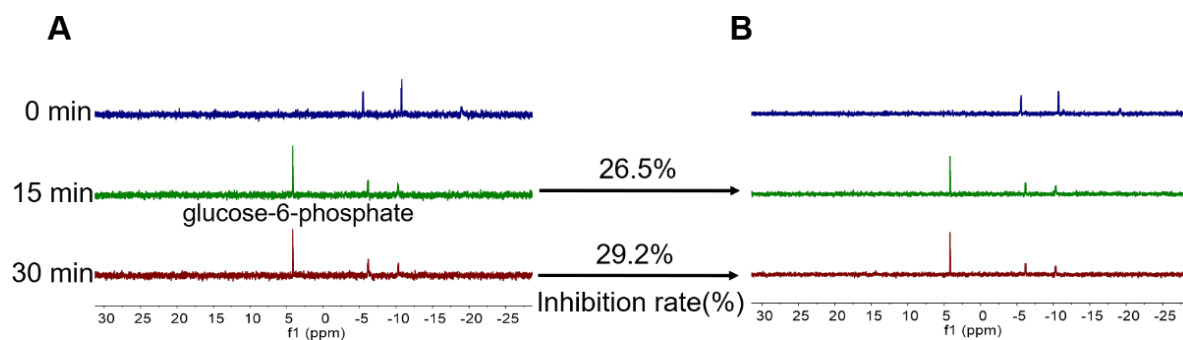


Fig. S8.  $^{31}\text{P}$  NMR screening for the HK inhibitor Lonidamine. Real-time  $^{31}\text{P}$  NMR spectra of glucose-6-Phosphate products catalyzed by HK (0.5 mg mL<sup>-1</sup>) in the presence of matching DMSO (A) or 200  $\mu\text{M}$  inhibitor Lonidamine (B).